Development 138, 4627-4638 (2011) doi:10.1242/dev.071464

JAK/Stat signaling regulates heart precursor diversification in *Drosophila*

Aaron N. Johnson[1], Mayssa H. Mokalled[1], Tom N. Haden[1] and Eric N. Olson[1,*]

SUMMARY

Intercellular signal transduction pathways regulate the NK-2 family of transcription factors in a conserved gene regulatory network that directs cardiogenesis in both flies and mammals. The *Drosophila* NK-2 protein Tinman (Tin) was recently shown to regulate *Stat92E*, the Janus kinase (JAK) and Signal transducer and activator of transcription (Stat) pathway effector, in the developing mesoderm. To understand whether the JAK/Stat pathway also regulates cardiogenesis, we performed a systematic characterization of JAK/Stat signaling during mesoderm development. *Drosophila* embryos with mutations in the JAK/Stat ligand *upd* or in *Stat92E* have non-functional hearts with luminal defects and inappropriate cell aggregations. Using strong *Stat92E* loss-of-function alleles, we show that the JAK/Stat pathway regulates *tin* expression prior to heart precursor cell diversification. *tin* expression can be subdivided into four phases and, in *Stat92E* mutant embryos, the broad phase 2 expression pattern in the dorsal mesoderm does not restrict to the constrained phase 3 pattern. These embryos also have an expanded pericardial cell domain. We show the E(spl)-C gene *HLHm5* is expressed in a pattern complementary to *tin* during phase 3 and that this expression is JAK/Stat dependent. In addition, *E(spl)-C* mutant embryos phenocopy the cardiac defects of *Stat92E* embryos. Mechanistically, JAK/Stat signals activate E(spl)-C genes to restrict Tin expression and the subsequent expression of the T-box transcription factor H15 to direct heart precursor diversification. This study is the first to characterize a role for the JAK/Stat pathway during cardiogenesis and identifies an autoregulatory circuit in which *tin* limits its own expression domain.

KEY WORDS: E(spl)-C, JAK/Stat, Cardiogenesis, *Drosophila*

INTRODUCTION

Intercellular signal transduction pathways provide positional information and guidance cues to effect the dynamic cellular changes driving organogenesis. In *Drosophila*, the Decapentaplegic (Dpp), Wingless (Wg) and Fibroblast growth factor (FGF) signaling pathways activate a highly conserved, cardiac-specific gene regulatory network by inducing the expression of the transcription factor *tin* in the precardiac, dorsal mesoderm (Olson, 2006). Tin activates the expression of transcription factors in the GATA (Klinedinst and Bodmer, 2003), T-box (Qian et al., 2005a; Reim et al., 2005) and Hand (Han and Olson, 2005) protein families that, in turn, direct cell fate specification and induce muscle structural genes. Although the key components of this cardiac-specific gene regulatory network have been characterized, the precise mechanisms by which Tin regulates cardiac cell diversification are only partially understood.

A genome-wide analysis of Tin binding sites identified novel Tin target genes that probably specify diverse cell fates in the mesoderm (Liu et al., 2009). Of the 400 binding sites reported, two loci, *eyes absent* and *Stat92E*, were shown to be direct Tin target genes. Stat92E is the transcriptional effector of the JAK/Stat pathway and, although the JAK/Stat pathway is one of a few conserved signal transduction pathways in Metazoa, a role for JAK/Stat signaling during cardiac morphogenesis has not been described. The identification of Stat92E as a Tin-regulated transcription factor suggests that the JAK/Stat pathway could be a component of the cardiac-specific gene regulatory network.

[1]Department of Molecular Biology, UT Southwestern Medical Center at Dallas, 5323 Harry Hines Boulevard, Dallas, TX 75390-9148, USA.
*Author for correspondence (eric.olson@utsouthwestern.edu)

Accepted 22 August 2011

In *Drosophila*, the canonical intracellular JAK/Stat response is initiated when an Unpaired (Upd; Os – Flybase) ligand binds the transmembrane receptor Domeless (Dome) (Hou et al., 2002). The *Drosophila* genome encodes three *upd* paralogs. Upd and Upd2 have overlapping segmental expression patterns during mesoderm development and, because both ligands signal through Dome in the wing, these proteins are thought to have redundant functions (Hombria et al., 2005). Upon ligand binding, Dome activates a receptor-associated JAK (Hopscotch) that, in turn, phosphorylates preassociated Stat (Stat92E) dimers (Novak et al., 1998; Stancato et al., 1996). Phosphorylated Stat92E homodimers translocate to the nucleus to regulate the expression of specific target genes.

The expression patterns of Upd and Upd2 have probably precluded previous studies of the JAK/Stat pathway during *Drosophila* heart development. Upd and Upd2 are expressed from the ventral ectoderm, which is relatively distant from the *tin* expression domain in the dorsal mesoderm, during a brief developmental window (Hombria et al., 2005; Karsten et al., 2002). However, the pulse of Upd and Upd2 expression in the ventral ectoderm is coincident with a dynamic spatial change in *tin* expression.

tin expression can be divided into four distinct spatial-temporal phases. Phase 1 *tin* expression initiates after gastrulation during which Twist (Twi) activates pan-mesodermal *tin* expression via the enhancer tinB (Yin et al., 1997). Phase 2 begins after FGF-mediated mesoderm spreading in which Dpp signals produced by the dorsal ectoderm maintain *tin* expression throughout the dorsal mesoderm via a second enhancer, tinD (Xu et al., 1998). It is during phase 2 that Tin specifies the major dorsal mesoderm derivatives. Phase 3 initiates after dorsal mesoderm progenitor specification and is characterized by a pronounced restriction of *tin* to the cardiac and visceral muscle progenitors. Upd and Upd2 are expressed in the ventral ectoderm during the transition from phase

2 to phase 3 expression. Phase 4 initiates after precursor specification and is characterized by further restriction of *tin* to the cardiac precursors that give rise to the contractile cardiomyocytes and the noncontractile pericardial nephrocytes. Phase 4 expression further directs heart cell diversification and maturation and is dependent on a third enhancer element, tinC (Venkatesh et al., 2000; Zaffran et al., 2006).

To understand whether the JAK/Stat pathway influences cardiac morphology, we performed a systematic characterization of JAK/Stat signaling during mesoderm development. *upd* and *Stat92E* embryos have non-functional hearts characterized by a dysfunctional lumen, cell-cell adhesion defects and inappropriate cell aggregations. We show that the JAK/Stat pathway is active in the dorsal mesoderm during the transition from phase 2 to phase 3 *tin* expression, and that JAK/Stat signals are necessary to restrict *tin* expression. *Stat92E* embryos also show an expanded pericardial cell domain owing to inappropriate heart precursor diversification during phase 3. The E(spl)-C gene *HLHm5* is expressed in a pattern complementary to *tin* in the dorsal mesoderm and is JAK/Stat dependent. In addition, *E(spl)-C* mutant embryos phenocopy the cardiac defects we observe in *Stat92E* embryos. This study is the first to show that the JAK/Stat pathway regulates heart development and that *tin* restricts its own expression in the dorsal mesoderm via a novel regulatory circuit.

MATERIALS AND METHODS

Drosophila genetics

All stocks were obtained from the Bloomington Stock Center unless otherwise noted. The stocks used in this study were: upd^{4}, FRT.82B $Stat92E^{85C9}$, FRT.82B $Stat92E^{397}$ (Silver and Montell, 2001), UAS.Stat92E-HA (Ekas et al., 2006), hs.Flp, FRT.82B ovo^{D1}, Twi.Gal4, 24B.Gal4, En.Gal4, HLHm5.lacZ, m4.lacZ, E(spl).lacZ, Df(3R)Espl22, Df(3R)Espl$^{\Delta md\text{-}m6}$ (Bardin et al., 2010), UAS.Socs36E (Callus and Mathey-Prevot, 2002), Hand.Gal4 (Han and Olson, 2005) and UAS.Twi (Castanon et al., 2001). FM7i, Act.GFP; TM3, Twi.Gal4 2X-UAS.eGFP; and TM6B, AbdA.lacZ were used to identify homozygous embryos.

The crosses to generate GLC experimental embryos include:

Stat92E^{M-Z-}:

Hand.eGFP; FRT.82B $Stat92E^{85C9/397}$ /TM3, twi.eGFP × hs.Flp/+; FRT.82B $Stat92E^{85C9/397}$ /FRT.82B ovo^{D1}

Stat92E^{M-}rescue:

twi.Gal4 × hs.Flp/+; UAS-Stat92E-HA/+; FRT.82B $Stat92E^{85C9}$ /FRT.82B ovo^{D1}

twi.Gal4; 24B.Gal4 × hs.Flp/+; UAS-Stat92E-HA/+; FRT.82B Stat92E^{85C9} /FRT.82B ovo^{D1}

en.Gal4 × hs.Flp/+; UAS-Stat92E-HA/+; FRT.82B $Stat92E^{85C9}$ /FRT.82B ovo^{D1}

en.Gal4; 24B.Gal4 × hs.Flp/+; UAS-Stat92E-HA/+; FRT.82B $Stat92E^{85C9}$ /FRT.82B ovo^{D1}

HLHm5.lacZ:

HLHm5.lacZ × hs.Flp/+; FRT.82B $Stat92E^{85C9}$ /FRT.82B ovo^{D1}.

In situ hybridization, immunohistochemistry and imaging

Antibody staining and in situ hybridization were performed as described (Johnson et al., 2007). Antibodies used in this study were rabbit anti-Mef2 (Lilly et al., 1995), rabbit anti-Tin (Venkatesh et al., 2000), rabbit anti-Odd (Ward and Skeath, 2000), rabbit anti-GFP (Torrey Pines Laboratories), mouse anti-HA (Santa Cruz), mouse anti-βgal (Promega) and mouse anti-Fasciclin 3 (FasIII, Developmental Studies Hybridoma Bank). HRP-, Alexa488- or Alexa633-conjugated secondary antibodies were used to detect primary antibodies (Molecular Probes). The TSA system (Molecular Probes) was used to detect HRP-conjugated secondary antibodies. Mef2 was directly conjugated with Zenon633 (Molecular Probes) for co-labeling with rabbit primary antibodies. BDGP clone RE69770 (*HLHm5*) and IP01538 (*H15*) were used to generate in situ probes. The *m4* transcript was cloned from 0- to 24-hour-old embryo cDNA made with the Superscript III first-strand synthesis system (Invitrogen). Images were generated with LSM 510 (Zeiss) and DMRXE (Leica) microscopes. Wild-type and mutant embryos were prepared and imaged in parallel where possible.

Chromatin immunoprecipitation

Four- to six-hour-old embryos expressing Stat92E-HA under the control of Twi.gal4, 24B.gal4 were collected, dechorionated, cross-linked, devitellinated and homogenized as described (Sandmann et al., 2006). The remainder of the immunoprecipitation was performed with the EZ-ChIP system per manufacturer's specification (Millipore). Chromatin was precipitated with or without 5 μg of anti-HA for the negative control, PCR amplified, and quantified by standard methods using ImageJ 1.40g software.

Quantitative real-time PCR

Four- to six-hour-old embryos were collected and homogenized in TRizol (Invitrogen) and RNA was extracted per manufacturer's specification. cDNA was generated using Superscript III and qPCR was performed with SYBR Green (Promega) using an ABI Prism 7000. Primers were designed to span introns for all intron-containing transcripts. qPCR reactions were run in triplicate and normalized to *RpL32* expression.

RESULTS

As Tin regulates *Stat92E* during mesoderm development (Liu et al., 2009), we speculated that the JAK/Stat pathway could be a component of the cardiac-specific gene regulatory network. To test this hypothesis, we characterized cardiac morphology in embryos mutant for the JAK/Stat ligand *upd*. The reporter gene Hand.GFP expresses a nuclear-localized GFP in the dorsal vessel (Fig. 1A) and serves as a useful tool to identify novel regulators of cardiac development (Yi et al., 2008). Using Hand.GFP as a marker, we found that a subset of *upd* embryos showed incomplete heart tube formation due to the loss of cell-cell adhesion among cardioblasts (38.1%, n=21; Fig. 1B). The incomplete phenotypic penetrance in *upd* embryos probably reflects functional redundancy with *upd2*. In addition, all embryos maternal and zygotic mutant for two distinct *Stat92E* loss-of-function alleles (hereafter $Stat92E^{M-Z-}$) showed cardiac defects similar to those of *upd* embryos (100% n≥24; Fig. 1C,D). Cardiogenesis is, therefore, dependent on JAK/Stat signaling.

The JAK/Stat pathway does not regulate cardioblast cell polarity, cardioblast cell survival or dorsal closure

The cardiac defects in $Stat92E^{M-Z-}$ embryos suggested that the JAK/Stat pathway might regulate cardiac morphology late in embryogenesis. Cardioblasts originate as unpolarized mesenchymal cells that generate a unique cell polarity after epithelial transition to complete cardiac tube morphogenesis. Embryos that fail to generate proper cardioblast cell polarity, such as *slit* and *robo* mutant embryos, show cardiac defects similar to those found in $Stat92E^{M-Z-}$ embryos (Qian et al., 2005b). We used FasIII to assay cell polarity and found that cardioblast cell polarity is normal in $Stat92E^{M-Z-}$ embryos (see Fig. S1 in the supplementary material). We then investigated whether the cardiac defects in $Stat92E^{M-Z-}$ embryos are secondary to dorsal closure defects but found $Stat92E^{M-Z-}$ embryos complete dorsal closure normally (see Fig. S1 in the supplementary material). A third potential explanation for the cardiac defects in $Stat92E^{M-Z-}$ embryos is that the JAK/Stat pathway promotes cardioblast cell survival. However, using TUNEL staining, we saw no apoptotic cardioblasts in wild-type (WT) or $Stat92E^{M-Z-}$ embryos (see Fig. S1 in the supplementary material). Because JAK/Stat signaling does not coordinate

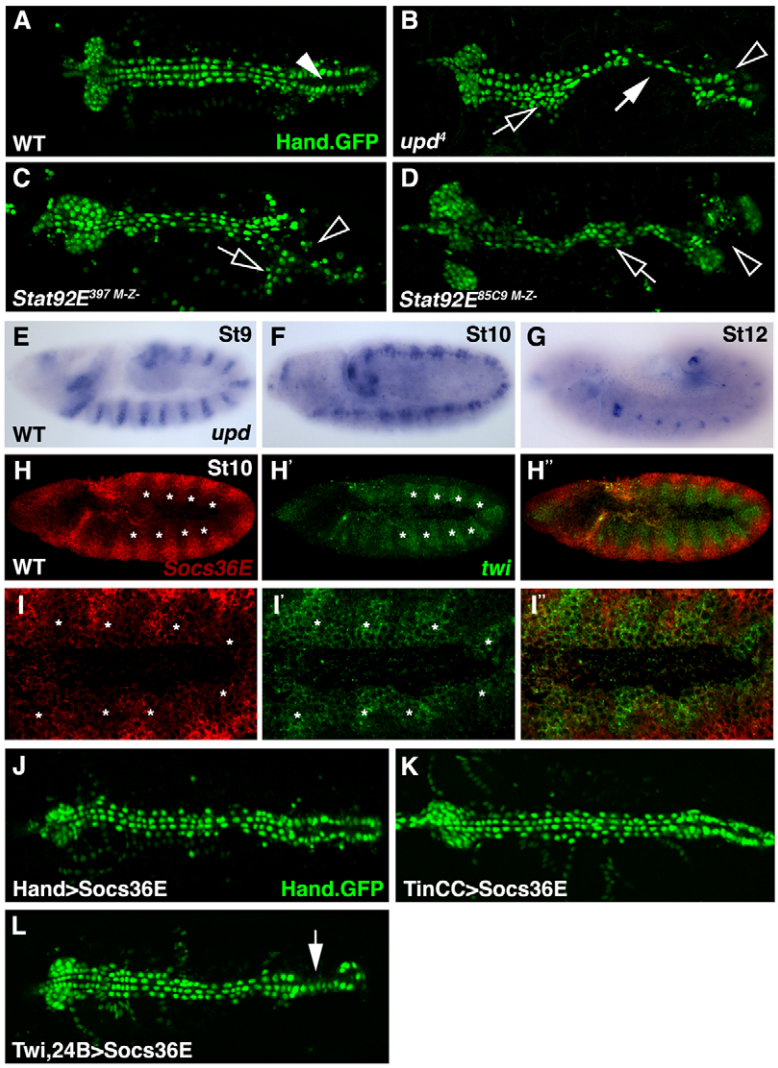

Fig. 1. The Jak/Stat pathway regulates cardiac morphology and is active in the dorsal mesoderm during cardiac precursor specification. (**A**) WT Hand.GFP embryos express nuclear-localized GFP throughout the dorsal vessel. The contractile 'heart' (arrowhead) positioned at the posterior of the dorsal vessel pumps hemolymph through the anterior aorta. (**B**) Zygotic *upd*^{4} embryos lose cardioblast cell-cell adhesion (white arrow) causing inappropriate cell aggregations (open arrow) and incomplete heart lumen formation (open arrowhead). (**C**,**D**) Embryos maternal and zygotic mutant for *Stat92E*^{397} (C) or *Stat92E*^{85C9} (D) phenocopy the dorsal vessel defects of *upd* embryos. (**E-G**) *upd* mRNA expression in WT embryos. *upd* expression in the ventral ectoderm is segmented during St9 (E). *upd* expression is restricted to the tracheal system and hindgut in St10 (F) and St12 (G) embryos. (**H-I"**) St10 WT embryo double labeled for *Socs36E* (red) and *twi* (green) mRNA. *Socs36E* and *twi* expression is complementary in the dorsal mesoderm. Regions of the mesoderm segment expressing high levels of *twi* (asterisks) express low levels of *Socs36E*. (**J**,**K**) St17 embryos expressing Hand.GFP. Expressing Socs36E in the heart after cardioblast precursor specification using Hand.gal4 (J) or TinCC.gal4 (K) does not affect heart morphology. (**L**) Expressing Socs36E in the heart prior to cardioblast precursor specification using Twi.gal4, 24B.gal4 induces mild cardioblast cell-cell adhesion defects. A-G show dorsal views of Hand.GFP expression in live St17 embryos. Embryos are oriented with anterior to the left.

cardioblast cell polarity, dorsal closure or cardioblast cell survival, we speculated that JAK/Stat signaling might regulate cardiac development during the early stages of embryogenesis.

The JAK/Stat pathway is active in the dorsal mesoderm

To identify the spatial and temporal requirement of the JAK/Stat pathway during mesoderm development, we assayed *upd* expression over the course of embryogenesis. Although the *upd* expression pattern has been described (Karsten et al., 2002), we expected close examination of *upd* in the context of heart development to reveal expression in the dorsal ectoderm or the dorsal mesoderm. Unexpectedly, we could not detect *upd* in these tissues during any stage of development. However, brief segmental *upd* expression was detectable in the ventral ectoderm during St9 (Fig. 1E). In St10-12 embryos, *upd* was expressed in the developing tracheal system and the hindgut but was no longer detectable in the ventral ectoderm (Fig. 1F,G). These results, in combination with the cardiac defects we observed in *upd* embryos, suggest that Upd expressed in the ventral ectoderm might signal to cells in the precardiac dorsal mesoderm to regulate heart development.

A standard method to detect JAK/Stat pathway activity is to assay the expression of the Stat92E target gene *Socs36E* (Baeg et al., 2005). A previous study reported segmental *Socs36E* expression in the visceral but not in the dorsal mesoderm of St10 embryos (Liu et al., 2009) in a pattern similar to *twi*. To define accurately the relative dorsal-ventral and anterior-posterior position of the *Socs36E* expression domain, we performed double fluorescent in situ hybridization with *Socs36E* and *twi*. We found that *Socs36E* is indeed expressed in the dorsal mesoderm of St10 embryos and that *Socs36E* and *twi* have complementary expression patterns (Fig. 1H,I). Strikingly, each mesoderm segment comprised one region that expresses high levels of *twi* and an opposing region that expressed high levels of *Socs36E* (Fig. 1H,I). We conclude that Upd, and perhaps Upd2, expressed from the ventral ectoderm, translocates to the dorsal mesoderm and activates a segmented JAK/Stat intracellular response.

To support the hypothesis that JAK/Stat signaling during St10 establishes proper cardiac morphology, we expressed Socs36E specifically in the dorsal vessel after St12. *Socs36E* is not only a Stat92E target gene but is also a negative regulator of JAK/Stat signaling (Callus and Mathey-Prevot, 2002). Expressing Socs36E throughout the heart with Hand.gal4 or in a subset of cardioblasts using TinCC.gal4 did not induce cardiac defects (Fig. 1J,K). Pan-mesodermal expression of Socs36E prior to St10 using Twi.gal4, 24B.gal4 did, however, induce a mild cardioblast cell-cell adhesion phenotype (Fig. 1L). Socs36E expression does not completely block JAK/Stat signaling and the strength of the Twi.gal4,

24B.gal4>Socs36E phenotype is consistent with that reported for other developmental contexts (Bach et al., 2003; Callus and Mathey-Prevot, 2002). Thus, JAK/Stat signaling to the dorsal mesoderm prior to St12 directs proper mesoderm development.

The JAK/Stat pathway regulates phase 3 *tin* expression

As the JAK/Stat pathway is active in the dorsal mesoderm during St10, we thought that JAK/Stat signaling might modulate the expression of genes that: (1) regulate cardiac precursor specification and (2) show dynamic expression during early mesoderm development. One obvious candidate was *tin* because the transition from broad phase 2 expression to restricted phase 3 expression is coincident with *Socs36E* expression in the dorsal mesoderm. By St11, the phase 3 *tin* expression pattern was evident as Tin-positive (Tin+) cells were juxtaposed with Tin-negative (Tin–) cells in the dorsal mesoderm (Fig. 2A). However, St11 *Stat92E*$^{M-Z-}$ embryos showed broad, unrestricted Tin expression throughout the dorsal mesoderm (Fig. 2B).

To confirm that the altered Tin expression pattern in *Stat92E*$^{M-Z-}$ embryos is mesoderm cell autonomous, we performed a rescue experiment by crossing UAS.Stat92E-HA/+; FRT82B *Stat92E*^{85C9}/

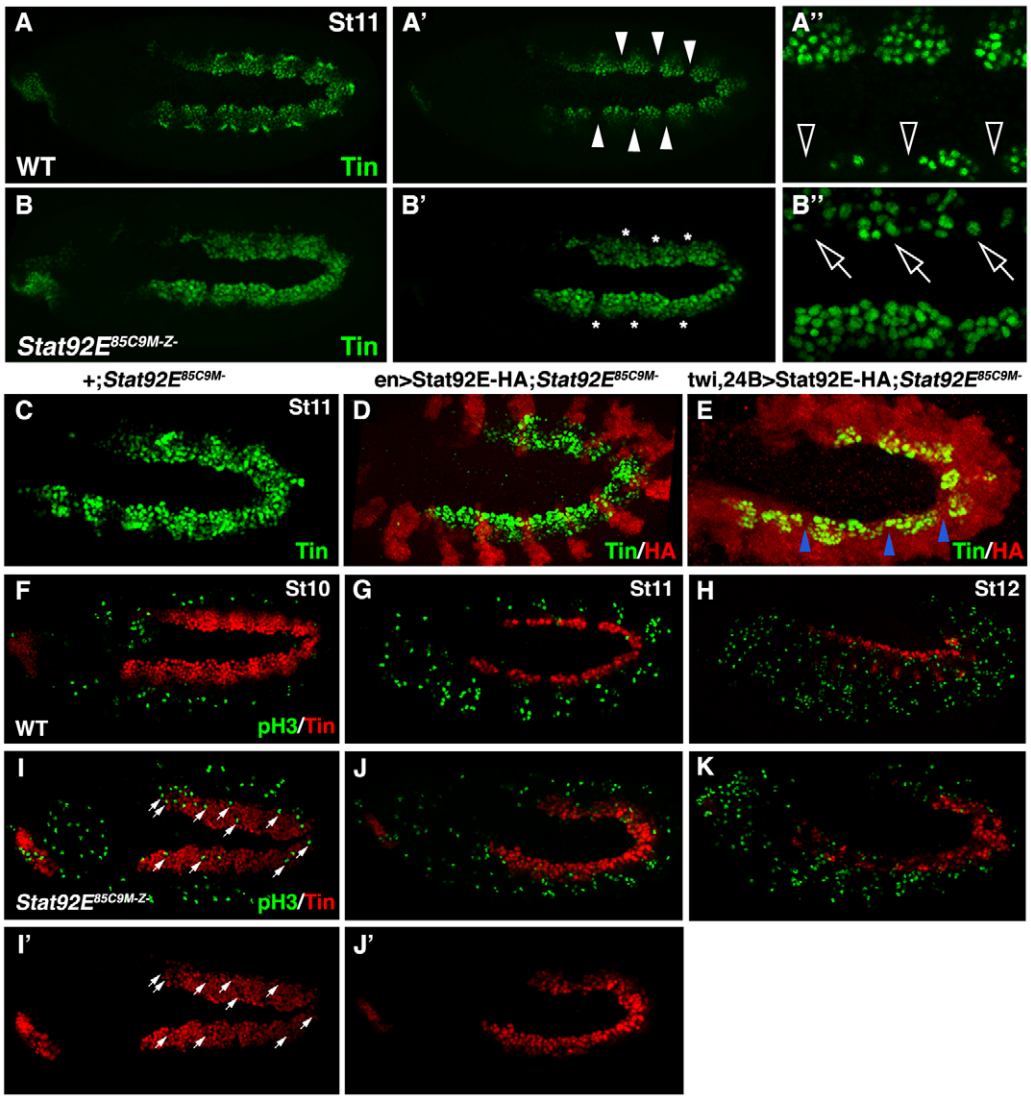

Fig. 2. JAK/Stat signaling restricts Tin expression in the dorsal mesoderm. (**A-B″**) Oblique views of St11 embryos labeled for Tin. The confocal micrographs in A and B include the entire Tin expression domain whereas the micrographs in A′, A″, B′ and B″ include only the dorsal mesoderm. (A,A′) Tin expression is restricted to the cardiac and visceral muscle progenitors in WT embryos. Note that Tin is not expressed in a subset of dorsal mesoderm cells (arrowheads). (B,B′) In *Stat92E*$^{M-Z-}$ St11 embryos, Tin expression does not restrict (asterisks). (A″,B″) High magnification micrographs show that the embryos are slightly rotated (oblique) giving a differential projection of the dorsal mesoderm. (A″) This scan captures more medially positioned Tin+ cells in the top of the image compared with the bottom. Note the large gaps between Tin+ cells in the dorsal-most mesoderm of WT embryos (open arrowheads). (B″) This scan captures more medially positioned Tin+ cells in the bottom of the image compared with the top. Tin-expressing cells can be identified throughout the dorsal-most mesoderm of *Stat92E*$^{M-Z-}$ embryos (open arrows). (**C-E**) St11 embryos labeled for HA and Tin. St11 *Stat92E*$^{M-}$ embryos (C) and *Stat92E*$^{M-}$ embryos that express Stat92E-HA in the ectoderm (D) show inappropriate Tin expression. *Stat92E*$^{M-}$ embryos that express Stat92E-HA in the mesoderm show restricted Tin expression (E; blue arrowheads). (**F-K**) Embryos labeled for pH3 and Tin. pH3 is not detectable in Tin+ cells of WT embryos during St10 (F), St11 (G) or St12 (H) or in *Stat92E*$^{MZ-}$ embryos at the same stages (I-K). pH3+ cells appear to be present in the Tin expression domain of *Stat92E*$^{MZ-}$ embryos; however, a majority of these nuclei do not co-express Tin and are likely to be in the ectoderm (arrows). Embryos are oriented with anterior to the left.

FRT82B ovoD1 females to males homozygous for an ectoderm driver (En.Gal4) or a strong mesoderm driver (Twi.Gal4, 24B.Gal4). In this crossing scheme, all embryos lack the maternal contribution of *Stat92E* (*Stat92E^{M-}*), but only half of the embryos express the Stat92E-HA transgene. *Stat92E^{M-}* embryos that do not express Stat92E-HA or that express Stat92E-HA in the ectoderm failed to restrict Tin expression in the dorsal mesoderm (Fig. 2C,D). By contrast, *Stat92E^{M-}* embryos that express Stat92E-HA in the mesoderm showed a restricted Tin expression domain that was comparable to WT embryos (Fig. 2E). Thus, cells of the dorsal mesoderm transduce JAK/Stat signals to appropriately refine *tin* expression.

Because the JAK/Stat pathway also regulates cell division (Hou et al., 2002), we assayed phosphorylated Histone3 (pH3; His – FlyBase) as a marker of cell proliferation. Neither WT nor *Stat92E^{M-Z-}* embryos accumulated pH3 in Tin+ cells prior to or after the restriction of *tin* in the dorsal mesoderm (Fig. 2F-K). JAK/Stat signaling, therefore, regulates gene expression, and not cell proliferation, to restrict *tin* in the dorsal mesoderm.

Jak/Stat signals regulate pericardial cell number

We next wanted to understand whether the JAK/Stat pathway regulates the specification or the diversification of heart precursor cells. The *Tbx20* ortholog *midline* (*mid*) is regulated by Tin in differentiating cardioblasts and is a useful marker of precursor diversification (Fig. 3A). *Stat92E^{M-Z-}* embryos showed normal *mid* expression in the dorsal mesoderm throughout embryogenesis, suggesting that cardioblasts differentiate appropriately in the absence of JAK/Stat signals (Fig. 3B-F). A second indicator of cell fate specification and diversification in the dorsal vessel is the expression of Tin itself. After germ band retraction, embryonic segments A2-A7 contain six cardioblasts, four of which express Tin (Fig. 3G). At this stage, Tin is also expressed in a subset of pericardial cells positioned ventral to the cardioblasts. St13 *Stat92E^{M-Z-}* embryos expressed Tin in four cardioblasts per hemisegment, but showed a significant increase in the number of Tin+, Mef2– pericardial cells (Fig. 3H,M,N). To confirm that the ectopic Tin+ cells in *Stat92E^{M-Z-}* embryos are indeed pericardial cells, we looked at the expression of Pericardin (Prc), an extracellular matrix protein expressed in all pericardial cells of St16 embryos. The Prc expression domain was expanded in *Stat92E^{M-Z-}* embryos and ectopic Tin+ cells co-expressed Prc (Fig. 3I,J). A third pericardial cell marker, Odd-skipped (Odd), was expressed in Tin– pericardial cells and we found that the number of Odd+ pericardial cells was also significantly increased in *Stat92E^{M-Z-}* embryos at St13 (Fig. 3K,L,O). Interestingly, *Stat92E^{M-Z-}* embryos also showed a reduced number of somatic muscle founder cells and a smaller visceral muscle domain (see Fig. S2 in the supplementary material). Therefore, proper diversification of heart progenitors requires Stat92E-mediated regulation of *tin* expression.

We then extended our rescue experiments to assay Tin+ pericardial cell specification. In *Stat92E^{M-}* embryos, the number of Tin+ cells was significantly greater than that in WT embryos at St13 (Fig. 4A-E) however, *Stat92E^{M-}* embryos that express Stat92E-HA in the mesoderm did not show a significant difference in the number of Tin+ cells compared with WT embryos (Fig. 4A′,B′,D′). By contrast, *Stat92E^{M-}* embryos that express Stat92E-HA solely in the ectoderm showed a significant increase in the number of Tin+ cells (Fig. 4C′). Therefore, expression of Stat92E in the mesoderm is sufficient to rescue the pericardial cell phenotype in *Stat92E^{M-}* embryos. Surprisingly, expressing Stat92E-HA in either the mesoderm or the ectoderm of *Stat92E^{M-}* embryos did not fully rescue cardioblast cell-cell adhesion defects (Fig. 4A‴-C‴). *Stat92E^{M-}* embryos that express Stat92E-HA in both the mesoderm and the ectoderm showed reduced cardiac cell adhesion defects (Fig. 4D‴). The heart tube formation defects in *Stat92E^{M-}* embryos therefore reflect the pleiotropic functions of the JAK/Stat pathway outside the mesoderm. For example, JAK/Stat signaling regulates segmentation (Harrison et al., 1998), ectoderm morphogenesis (Bertet et al., 2009) and the development of ectoderm derivatives, including the tracheal system (Sotillos et al., 2010). Incomplete ectoderm development probably exacerbates the mesoderm patterning defects in *Stat92E^{M-}* embryos, causing incomplete cardiac morphogenesis.

E(spl)-C gene expression is dependent on JAK/Stat signaling

The modENCODE project performed a Stat92E chromatin immunopurification (ChIP)-chip analysis on 0- to 12-hour-old embryos (Celniker et al., 2009) and identified three Stat92E binding regions proximal to the *Socs36E* locus, including the known Stat92E Response Element (Baeg et al., 2005). The ChIP-chip analysis identified additional Stat92E target genes including *ventral veins lacking* and *trachealess* (Sotillos et al., 2010) (see Table S1 in the supplementary material), suggesting that the ChIP-chip data would be a useful tool to identify Stat92E target genes in the mesoderm. Although a total of 107 loci fall within 10 kb of a reported Stat92E binding region (see Table S1 in the supplementary material), the *tin* transcriptional start site is over 262 kb from the closest Stat92E binding region (3R:17466843). Thus, Stat92E probably regulates *tin* expression indirectly.

Nine of the 107 loci identified by the ChIP-chip analysis are known regulators of mesoderm development, including components or targets of the Dpp, Hedgehog and Notch signaling pathways (*tkv*, *shn*, *hh*, *H*, *ed*, *th*, *numb*, *mid* and *m4*). We collected RNA from WT and *Stat92E^{M-}* 4- to 6-hour-old embryos, performed quantitative RT-PCR (qPCR), and found that the E(spl)-C gene *m4* was the most downregulated of the nine candidate genes (Fig. 5B). The E(spl)-C genes encode members of the HLH and Bearded family of transcription factors and are well characterized Notch targets that regulate *twi* expression (Delidakis and Artavanis-Tsakonas, 1992; Lai et al., 2000; Tapanes-Castillo and Baylies, 2004). We checked the expression of the remaining E(spl)-C genes and found that, with the exception of *mα*, all of the E(spl)-C genes were significantly downregulated in *Stat92E^{M-}* embryos (Fig. 5C). Thus, E(spl)-C gene expression requires JAK/Stat signaling during the early stages of embryonic development.

The JAK/Stat pathway activates *HLHm5* expression in the dorsal mesoderm

To identify the E(spl)-C gene(s) that are expressed in the dorsal mesoderm during phase 3 *tin* expression, we assayed the activity of *m4*, *HLHm5* and *E(spl)* reporter genes in St11 embryos (Fig. 5A). Strikingly, HLHm5.lacZ directed *lacZ* expression specifically in Tin– cells of the dorsal mesoderm (Fig. 5D). Expression from HLHm5.lacZ is also detectable in the ventral mesoderm and neuroectoderm. In *Stat92E^{M-}* embryos, expression from HLHm5.lacZ was reduced throughout the embryo and completely absent from the dorsal mesoderm (Fig. 5E). Moreover, the regions of the dorsal mesoderm that should express HLHm5.lacZ instead expressed Tin in *Stat92E^{M-}* embryos. By contrast, E(spl).lacZ directs broad *lacZ* expression in the dorsal mesoderm, whereas m4.lacZ did not drive *lacZ* expression in the dorsal mesoderm of WT embryos (see Fig. S3 in the supplementary material).

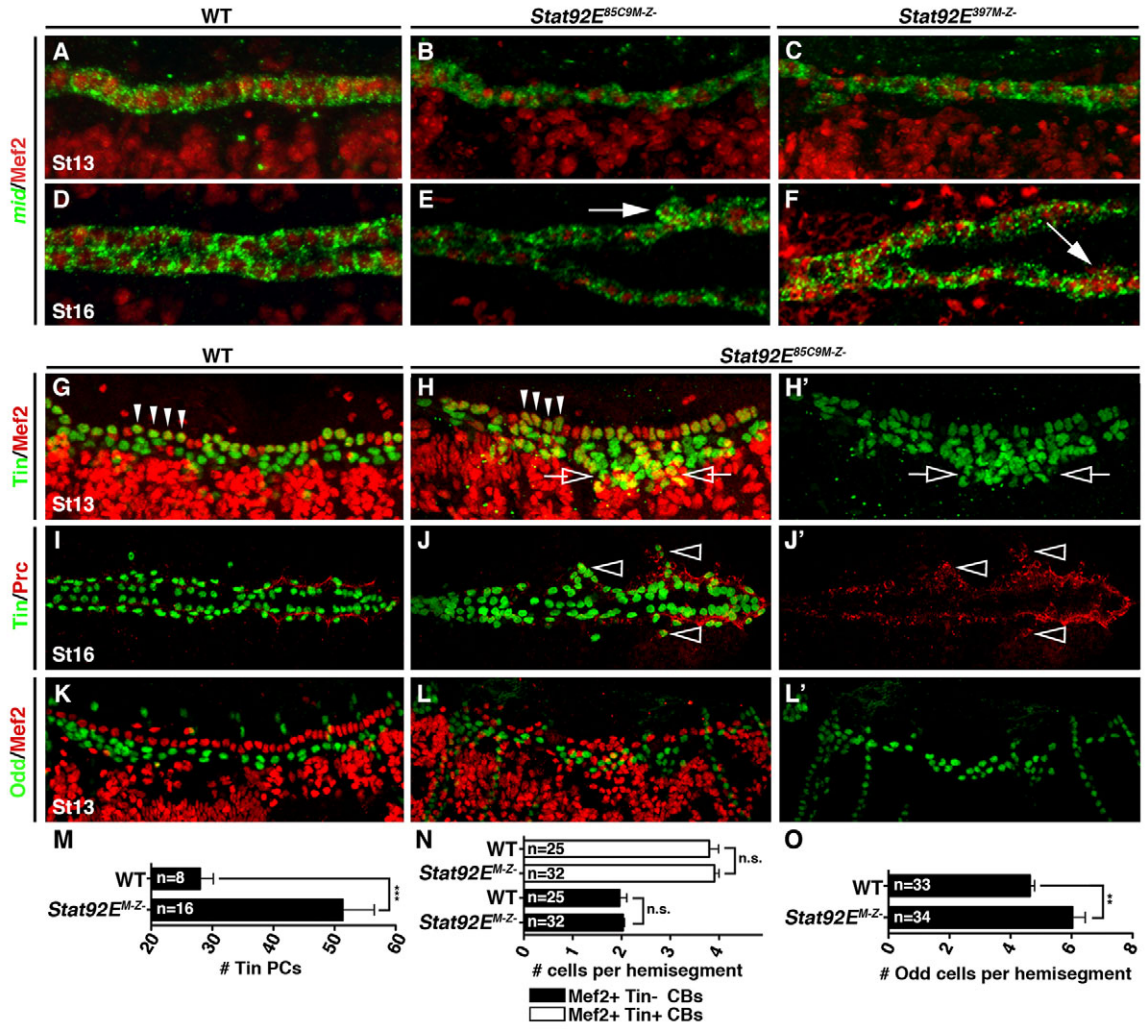

Fig. 3. JAK/Stat signaling regulates pericardial cell number. (**A-F**) Lateral views of St13 (A-C) and dorsal views of St16 (D-F) embryos labeled for Mef2 protein and *mid* mRNA. WT and *Stat92E*$^{M-Z-}$ embryos express *mid* in all Mef2+ cardioblasts by St13. *mid* expression persists to St16 even in the aggregated cardioblasts of *Stat92E*$^{M-Z-}$ embryos (arrows). (**G-H'**) Lateral views of St13 embryos labeled for Tin and Mef2. (G) WT St13 embryos express Tin in four cardiomyocytes per heart hemisegment (arrowheads) and in a subset of pericardial cells. Mef2 is not expressed in pericardial cells. (H) *Stat92E*$^{M-Z-}$ embryos express Tin in four cardiomyocytes in a majority of hemisegments but the number of Tin expressing pericardial cells is significantly increased (open arrows). (**I-J'**) Dorsal views of St16 embryos labeled for Tin and Prc. (I) Prc localizes to the extracellular matrix between cardiomyocytes and pericardial cells in WT embryos. (J) Ectopic Tin cells positioned lateral to the cardioblasts (open arrowheads) co-express Prc in *Stat92E*$^{M-Z-}$ embryos. (**K-L'**) Lateral views of St13 embryos labeled for Odd and Mef2. (K) WT embryos express Odd in four pericardial cells per hemisegment. (L) The number of Odd+ pericardial cells is significantly increased in *Stat92E*$^{M-Z-}$ embryos. (**M**) Quantification of Tin+ pericardial cells (PCs) in one half of the mesoderm at St13. Tin+ pericardial cells were identified by lack of Mef2 expression. (**N**,**O**) Segmental quantification of Tin+ and Tin– cardioblasts (CBs) at St13 (N) and Odd+ pericardial cells at St13 (O). $^{**}P<0.005$, $^{***}P<0.001$, unpaired *t*-test. n.s., non-significant. Error bars represent s.e.m. Embryos are oriented with anterior to the left.

Endogenous *HLHm5* expression in the mesoderm initiated at St10 as segmental stripes (Fig. 5F) and expanded to a robust, periodic pattern in the dorsal mesoderm by St11 (Fig. 5G). HLHm5.lacZ therefore recapitulates *HLHm5* expression in the dorsal mesoderm. In addition, *HLHm5* expression was remarkably similar to *Socs36E* during St10 (compare Fig. 1I with Fig. 5F). *HLHm5* expression did not initiate in the dorsal mesoderm of *Stat92E*$^{M-}$ embryos during St10 (Fig. 5H) and was absent from the dorsal mesoderm through St11 (Fig. 5I). We then characterized Tin expression in Df(3R)Espl$^{\Delta m\delta\text{-}m6}$ St11 embryos and found that Tin expression did not fully restrict in the dorsal-most mesoderm (Fig. 5J,K). Thus, Stat92E induces *HLHm5* expression in the Tin– cells of the dorsal mesoderm and E(spl)-C genes are necessary to restrict Tin expression.

Stat92E binds discrete regions of *E(spl)-C* in the mesoderm

The 50 kb genomic region encoding *E(spl)-C* houses a total of three, conserved Stat92E consensus binding sites (SCBS; Fig. 5A; see Fig. S3 in the supplementary material). To determine whether Stat92E binds regions of *E(spl)-C*, we expressed Stat92E-HA in the mesoderm and performed our own ChIP analysis on 4- 6-hour-old embryos. We first assayed Stat92E-HA binding to the Stat92E response element in *Socs36E* and to the region upstream of *m4* identified by the modENCODE ChIP-chip experiment (referred to here as SCBS3; Fig. 5A,L) and confirmed that Stat92E-HA bound both of these regions in the mesoderm. For negative controls, we assayed Stat92E-HA

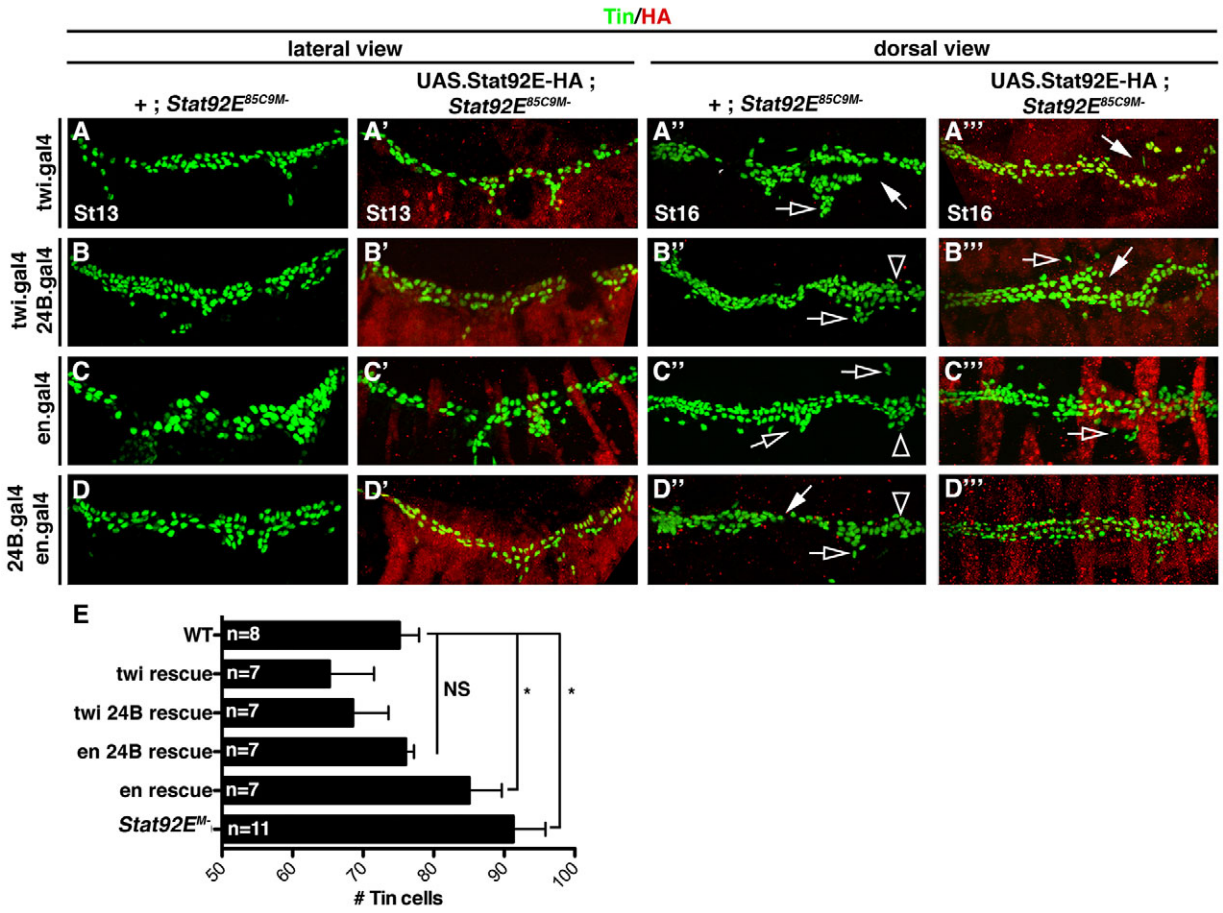

Fig. 4. JAK/Stat signaling in the mesoderm restricts pericardial cell number. Embryos labeled for HA and Tin. The crossing scheme is detailed in the text. (**A-D**) St13 embryos lacking the maternal contribution of *Stat92E* (*Stat92E*$^{M-}$) have an increased number of Tin+ cells compared with WT embryos. (**A′**,**B′**,**D′**) *Stat92E*^{M} embryos that express Stat92E-HA in the mesoderm show WT levels of Tin+ cells. (**C′**) *Stat92E*$^{M-}$ embryos that express Stat92E-HA in the ectoderm show a significant increase in the number of Tin+ cells compared with WT embryos. (**A″-D″**) St16 *Stat92E*$^{M-}$ embryos show a loss of cardioblast cell-cell adhesion (white arrows), collapsed 'heart' (open arrowheads) and inappropriate cell aggregations (open arrows). (**A‴-C‴**) *Stat92E*$^{M-}$ embryos that express Stat92E-HA in either the mesoderm or the ectoderm also show these three cardiac phenotypes, although they are less severe. (**D‴**) *Stat92E*$^{M-}$ embryos that express Stat92E-HA in the ectoderm and the mesoderm show mostly normal heart morphology. (**E**) Quantification of Tin+ cells in St13 embryos from the genotypes shown in A-D. **P*<0.05, unpaired *t*-test. NS, non-significant. Error bars represent s.e.m. Embryos are oriented with anterior to the left.

binding to an unconserved SCBS site upstream of *mα* (see Fig. S4 in the supplementary material) and to a highly conserved SCBS proximal to *hedgehog* (*hh*), expression of which is restricted to the ectoderm and the foregut endoderm in 4- to 6-hour-old embryos (see Fig. S4 in the supplementary material). Stat92E-HA did not bind regions near the *mα* or *hh* loci, suggesting that our ChIP experiments were identifying bona fide Stat92E chromatin-binding regions in the mesoderm. We then analyzed Stat92E-HA binding at two additional SCBS in *E(spl)-C* and found that Stat92E-HA binds SCBS1 but not SCBS2 in the mesoderm (Fig. 5L). Thus, *E(spl)-C* is a direct target of Stat92E in the mesoderm of 4- to 6-hour-old embryos. Although recent work in intestinal stem cells showed that the JAK/Stat pathway activates E(spl)-C genes (Jiang et al., 2009), this is the first evidence that *E(spl)-C* is a direct target of Stat92E.

Although Stat92E-HA binds regions of *E(spl)-C*, we did not identify an SCBS in the sequence comprising HLHm5.lacZ. Because *E(spl)-C* transcription factors regulate gene expression within *E(spl)-C* itself (Oellers et al., 1994), we conclude that Stat92E indirectly regulates *HLHm5* by regulating other E(spl)-C genes. Alternatively, Stat92E might directly regulate *HLHm5* via a non-consensus binding site(s).

E(spl)-C genes regulate heart morphology

E(spl)-C genes are known regulators of mesoderm development. Previous to our studies, two phenotypes have been reported in *E(spl)-C* mutant embryos: dysregulated *twi* expression in the mesoderm (Tapanes-Castillo and Baylies, 2004) and ectopic Ladybird+ cardiac progenitors (Jagla et al., 1997). To understand whether these phenotypes are related through a common mechanism, we characterized heart morphology in *E(spl)-C* mutant embryos and in embryos misexpressing Twi. Df(3R)Espl$^{\Delta m\delta\text{-}m6}$ deletes all the E(spl)-C genes from *HLHmdelta* to *m6* and presumably disrupts cis-regulatory sequences controlling *HLHm7* whereas Df(3R)Espl22 deletes *HLHm5*, *m6*, *HLHm7*, *E(Spl)* and *gro* (Fig. 5A). Embryos homozygous for Df(3R)Espl$^{\Delta m\delta\text{-}m6}$ (Fig. 6A) or transheterozygous for Df(3R)Espl$^{\Delta m\delta\text{-}m6}$/Df(3R)Espl22 (Fig. 6B) show cardiac phenotypes similar to *Stat92E*$^{M-Z-}$ embryos, including loss of

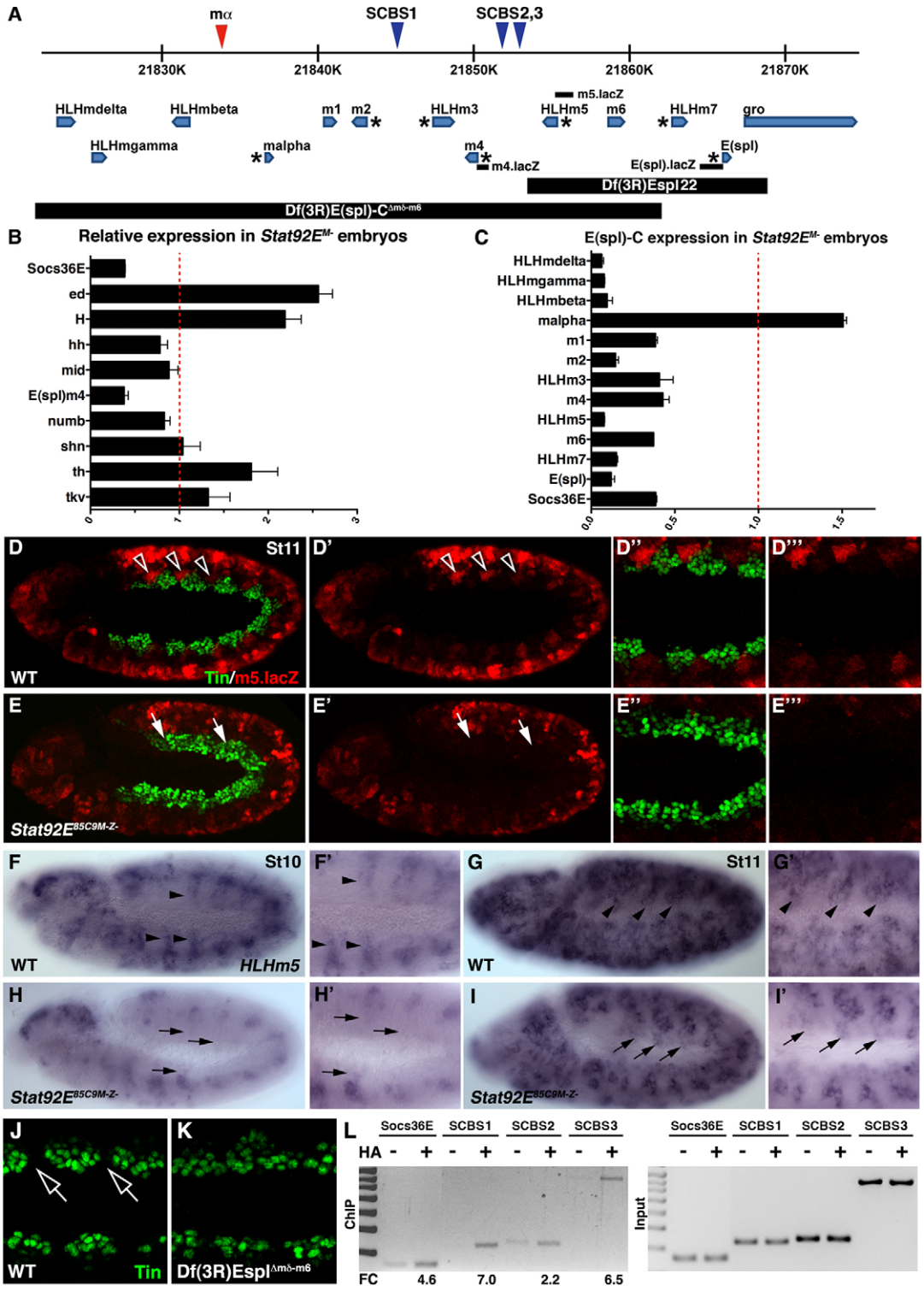

Fig. 5. See next page for legend.

cardioblast cell-cell adhesion. Thus, deletion of *HLHm5*, *m6*, and perhaps *HLHm7*, is sufficient to cause heart defects in St17 embryos. If the cardiac defects in E(spl)-C mutant embryos are solely due to dysregulated *twi* expression, then misexpressing Twi in the mesoderm should induce a cardiac phenotype similar to that of *E(spl)-C* embryos. Surprisingly, 24B>twi embryos do show a loss of cardioblast cell-cell adhesion (Fig. 6D), but these embryos also lack pericardial cells in the dorsal vessel.

E(spl)-C genes regulate pericardial cell number independently of *twi*

We then characterized Tin expression in 24B>twi and Df(3R)Espl$^{\Delta m\delta\text{-}m6}$ St13 embryos. Both 24B>twi and Df(3R)Espl$^{\Delta m\delta\text{-}m6}$ St13 embryos showed four Tin+ cardioblasts in a majority of hemisegments (Fig. 6D,E,K). However, Df(3R)Espl$^{\Delta m\delta\text{-}m6}$ embryos had an increased number of Tin+ pericardial cells compared with WT embryos, whereas 24B>twi

Fig. 5. Stat92E regulates *HLHm5* expression in the dorsal mesoderm. (**A**) The E(spl) gene complex. Blue triangles mark the position of conserved Stat consensus binding sites (SCBSs); the red triangle shows a non-conserved SCBS. E(spl)-C genes with previously reported mesoderm expression are marked with an asterisk. The position of the sequences comprising the m4.lacZ, HLHm5.lacZ and E(spl).lacZ reporters are shown. Sequences deleted by E(spl)-C deficiencies used in this study are indicated. (**B**,**C**) qPCR of extracts from 4- to 6-hour-old embryos showing relative mRNA expression in *Stat92E*$^{M-}$ embryos compared with WT. *Socs36E* and *m4* are downregulated in *Stat92E*$^{M-}$ embryos (B). With the exception of *mα*, all E(spl)-C genes are downregulated in *Stat92E*$^{M-}$ embryos (C). (**D-E‴**) St11 embryos double-labeled for HLHm5.lacZ and Tin. (D-D‴) WT embryos express HLHm5.lacZ in the neuroectoderm, lateral mesoderm and in the Tin- cells of the dorsal mesoderm (open arrowheads). (E-E‴) HLHm5.lacZ expression is dramatically reduced in St11 *Stat92E*$^{M-}$ embryos. *lacZ* is undetectable in the dorsal mesoderm of *Stat92E*$^{M-}$ embryos. (**F-I′**) *HLHm5* mRNA expression. In WT embryos, *HLHm5* expression initiates as stripes in the dorsal mesoderm during St10 (black arrowheads; F,F′) and expands to include large regions of the dorsal mesoderm by St11 (G,G′). *HLHm5* expression does not initiate in the dorsal mesoderm of *Stat92E*$^{M-}$ embryos by St10 (black arrows; H,H′) and is absent from the dorsal mesoderm at St11 (I,I′). (**J**,**K**) Oblique view of St11 embryos labeled for Tin similar in orientation to embryos in Fig. 2. Tin expression restricts in the dorsal-most mesoderm of WT embryos (J, open arrows) but not Df(3R)Espl$^{\Delta m\delta\text{-}m6}$ embryos (K). (**L**) Stat92E ChIP in 4- to 6-hour-old embryos. Stat92E-HA was expressed in the mesoderm with twi,24B.gal4. Cross-linked chromatin was immunoprecipitated with anti-HA or beads alone and PCR amplified. Stat92E binds SCBS1 and SCBS3 but not SCBS2 in the mesoderm. Stat92E does not bind a non-conserved consensus sequence between *mβ* and *mα* (see Fig. S4 in the supplementary material). Fold change (FC) was calculated using Image J. *Socs36E* served as a positive control. Error bars represent s.e.m. Embryos are oriented with anterior to the left.

embryos showed the appropriate number of Tin+ pericardial cells (Fig. 6E,L). Therefore, the role of E(spl)-C genes in regulating *twi* expression is independent from their role in regulating pericardial cell number.

Embryos misexpressing Twi in the mesoderm lack pericardial cells at St16 (Castanon et al., 2001); however, the correct number of Tin+ pericardial cells was specified at St13 (Fig. 6D). We assayed Tin expression in St16 24B>twi embryos and found a reduction in the number of Tin+ pericardial cells and Tin+ cardioblasts in the heart (Fig. 6F). By contrast, St16 Df(3R)Espl$^{\Delta m\delta\text{-}m6}$ embryos continued to show ectopic Tin+ pericardial cells (Fig. 6G). Therefore, embryos that misexpress Twi specify the correct number of heart precursors, but over the course of mesoderm migration, precursors are lost from the dorsal mesoderm. We favor a model in which dysregulated *twi* expression blocks heart precursor cell maturation, resulting in cell-cell adhesion defects during mesoderm migration.

The JAK/Stat pathway and the E(spl)-C genes restrict H15 expression

To gain insights into the mechanism by which JAK/Stat signaling and *E(spl)-C* regulate pericardial cell number, we assayed *H15* expression in *Stat92E*$^{M-Z-}$ and Df(3R)Espl$^{\Delta m\delta\text{-}m6}$ embryos. The T-box transcription factor H15 induces ectopic Tin+ cells when misexpressed in the mesoderm (Qian et al., 2005a). In St13 WT embryos, *H15* was expressed in a single row of cardioblasts in the dorsal mesoderm (Fig. 6H); however, multiple rows of dorsal mesoderm cells expressed *H15* in *Stat9292E*$^{M-Z-}$ and Df(3R)Espl$^{\Delta m\delta\text{-}m6}$ embryos (Fig. 6I,J). As neither *Stat92E*$^{M-Z-}$ (Fig. 3H) nor Df(3R)Espl$^{\Delta m\delta\text{-}m6}$ (Fig. 6E) embryos specifies supernumerary cardioblasts, we conclude that the JAK/Stat pathway activates E(spl)-C genes to limit the *H15* expression domain and, thus, the number of Tin+ pericardial cells.

DISCUSSION

To test the hypothesis that the JAK/Stat pathway functions in the cardiac-specific gene regulatory network, we performed a systematic characterization of JAK/Stat signaling during mesoderm development. We have shown that the JAK/Stat pathway regulates final cardiac morphology as well as heart precursor diversification. Our *Stat92E* loss-of-function analysis identified a discrete function for the JAK/Stat pathway in restricting *tin* during the transition from phase 2 to phase 3 expression. In addition, *Stat92E* embryos have an expanded pericardial cell domain arguing that the JAK/Stat pathway regulates *tin* to ensure proper heart precursor diversification. Mechanistically, we found that the E(spl)-C gene *HLHm5* is expressed in a complementary pattern to *tin* during phase 3 expression and that the JAK/Stat pathway activates *HLHm5* expression in the dorsal mesoderm. The E(spl)-C genes in turn repress *twi* expression to preserve cardiac morphology and restrict *tin* and *H15* expression to direct heart precursor diversification. These findings provide the first evidence of a role for the JAK/Stat pathway in cardiogenesis and identify a novel *tin* autoinhibitory circuit involving *Stat92E* and *E(spl)-C*.

Stat92E expression in the dorsal mesoderm

Stat92E is a direct Tin target gene during phase 2 expression; however, *Stat92E* is expressed in segmented stripes at this stage whereas *tin* is expressed throughout the dorsal mesoderm (Liu et al., 2009). In addition, embryos lacking only the maternal contribution of *Stat92E* have mesoderm patterning defects (Fig. 2C). Tin-regulated *Stat92E* zygotic transcription is therefore insufficient to coordinate mesoderm development. These data suggest that maternally contributed Stat92E is activated in response to segmented Upd and Upd2 activity, binds the *Stat92E* locus and co-activates *Stat92E* zygotic transcription with Tin (Fig. 7). In addition, ChIP-chip experiments identified Stat92E binding activity and a conserved SCBS within the Tin-responsive Stat92E mesoderm enhancer (see Table S1 and Fig. S4 in the supplementary material). We conclude that *Stat92E* and *tin* co-regulate a brief, spatially restricted JAK/Stat signaling event that patterns the mesoderm.

The *tin* autoinhibitory circuit

Phase 3 *tin* expression promotes cell-type diversification and differentiation within the dorsal mesoderm and is indirectly activated by Wg via the T-box transcription factors in the Dorsocross complex and the GATA factor Pannier (Jagla et al., 1997; Klinedinst and Bodmer, 2003; Reim and Frasch, 2005). A key finding of this study is that the JAK/Stat pathway activates the transcriptional repressor *HLHm5* in the dorsal mesoderm to establish phase 3 *tin* expression (Fig. 7). Because the *HLHm5* cis-regulatory region lacks a conserved SCBS, we predict that Stat92E regulates *HLHm5* expression through a non-consensus binding site. Alternatively, Stat92E acts at long distances to regulate gene expression (Sotillos et al., 2010). The SCBSs in *E(spl)-C* could be

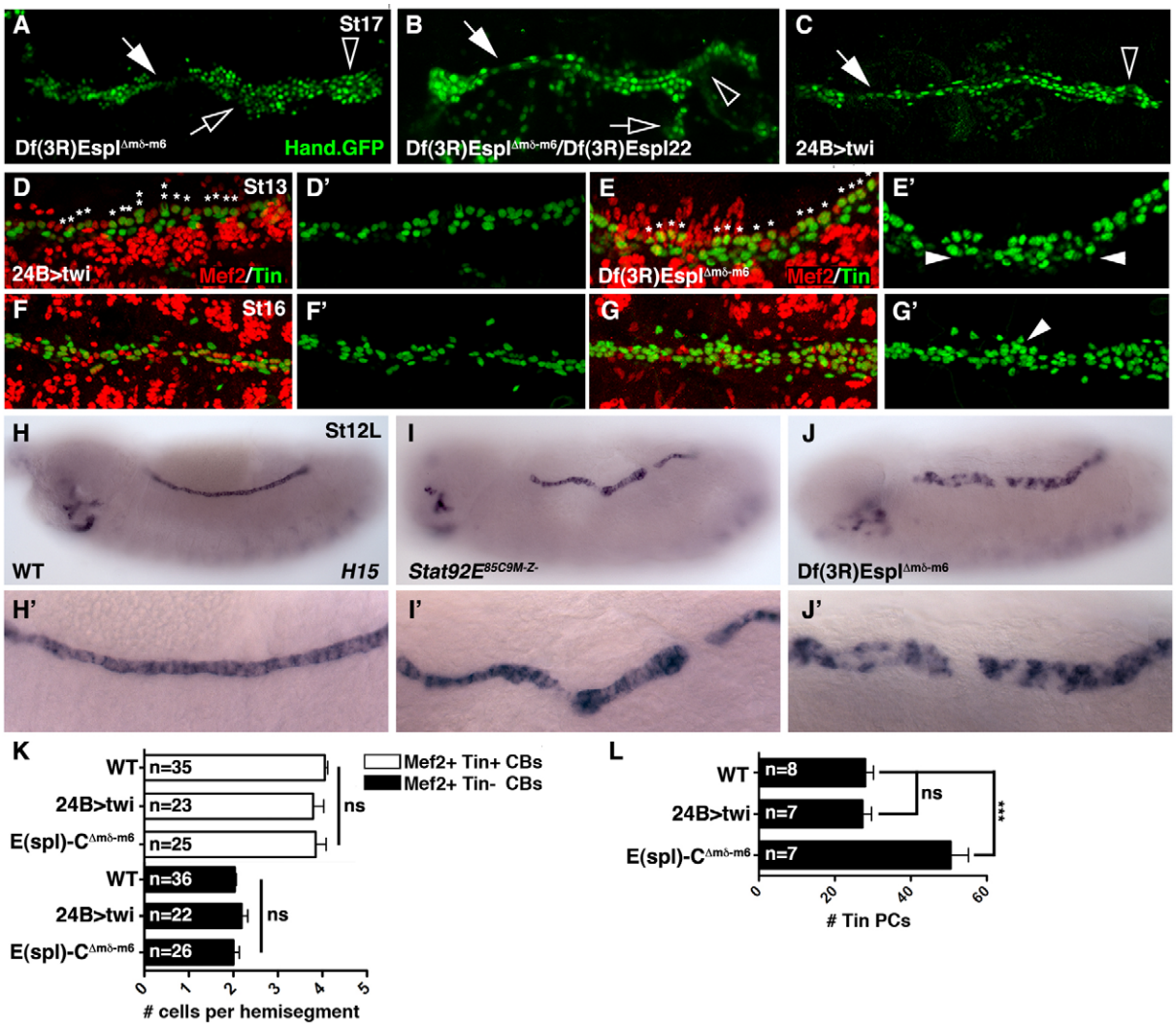

Fig. 6. *E(spl)-C* regulates cardiac morphology and pericardial cell number. (**A-C**) Dorsal views of Hand.GFP expression in live St17 embryos. Df(3R)Espl$^{\Delta m\delta\text{-}m6}$ homozygous embryos (A) and Df(3R)Espl$^{\Delta m\delta\text{-}m6}$/Df(3R)Espl22 heterozygous embryos (B) show cardiac phenotypes similar to *Stat92E^{M-Z-}* embryos including a collapsed 'heart' (open arrowheads), loss of cardioblast cell-cell adhesion (white arrows) and cell aggregations (open arrows). 24B>twi embryos (C) show a collapsed heart and loss of cardioblast cell-cell adhesion but not cell aggregations. Notice that Hand+ pericardial cells appear to be missing in 24B>twi embryos. (**D-G'**) Embryos double-labeled for Tin and Mef2. (F) 24B>twi St13 embryos have four Tin+ cells in a majority of hemisegments (asterisks). The number of Tin+ pericardial cells is comparable to WT. (E) Df(3R)Espl$^{\Delta m\delta\text{-}m6}$ St13 embryos also show a largely normal pattern of Tin+ cardioblasts; however, the number of Tin+ pericardial cells is increased compared with WT. (F) 24B>twi St16 embryos show a dramatic reduction in Tin+ cardioblasts and pericardial cells. (G) Df(3R)Espl$^{\Delta m\delta\text{-}m6}$ St16 embryos have ectopic Tin+ pericardial cells. (**H-J'**) *H15* mRNA expression in St13 embryos. WT embryos express *H15* in a single row of cardioblasts (H). *H15* expression expands ventrally in *Stat9292E^{M-Z-}* (I,I') and Df(3R)Espl$^{\Delta m\delta\text{-}m6}$ (J,J') embryos. (**K**) Segmental quantification of Tin+ and Tin– cardioblasts (CBs) at St13. (**L**) Quantification of Tin+ pericardial cells (PBs) in one half of the mesoderm at St13. Tin+ pericardial cells were identified by lack of Mef2 expression. ***P<0.001, unpaired t-test. ns, non-significant. Error bars represent s.e.m. Embryos are oriented with anterior to the left.

a platform from which Stat92E regulates multiple E(spl)-C genes that, in turn, regulate *HLHm5* expression. In either event, Stat92E-mediated activation of E(spl)-C genes restricts *tin* in the dorsal mesoderm to establish phase 3 expression. Tin, therefore, establishes an autoinhibitory circuit by activating its own repressors in the JAK/Stat pathway and in *E(spl)-C*.

Regulated *tin* expression directs heart precursor diversification

Both *Stat92E* and Df(3R)Espl$^{\Delta m\delta\text{-}m6}$ embryos show an increased number of Tin+ pericardial cells and an expanded *H15* expression domain (Fig. 2H, Fig. 6G,J-L). Misexpressing *mid* or *H15* in the mesoderm expands the number of Tin+ cells in the dorsal vessel (Qian et al., 2005a; Reim et al., 2005) and embryos misexpressing *mid* show a phenotype strikingly similar to *Stat92E* and *E(spl)* embryos (Reim and Frasch, 2005). As *mid*, and presumably *H15*, are positively regulated by Tin during St11/12 (Qian et al., 2005a), unrestricted *tin* expression in *Stat92E* or Df(3R)Espl$^{\Delta m\delta\text{-}m6}$ embryos expands the *H15* expression domain. Ectopic H15 then specifies supernumerary Tin+ pericardial cells. Because *mid* expression is not affected in *Stat92E* embryos, the expression of *mid* and *H15* must be controlled by distinct mechanisms and might have non-redundant functions.

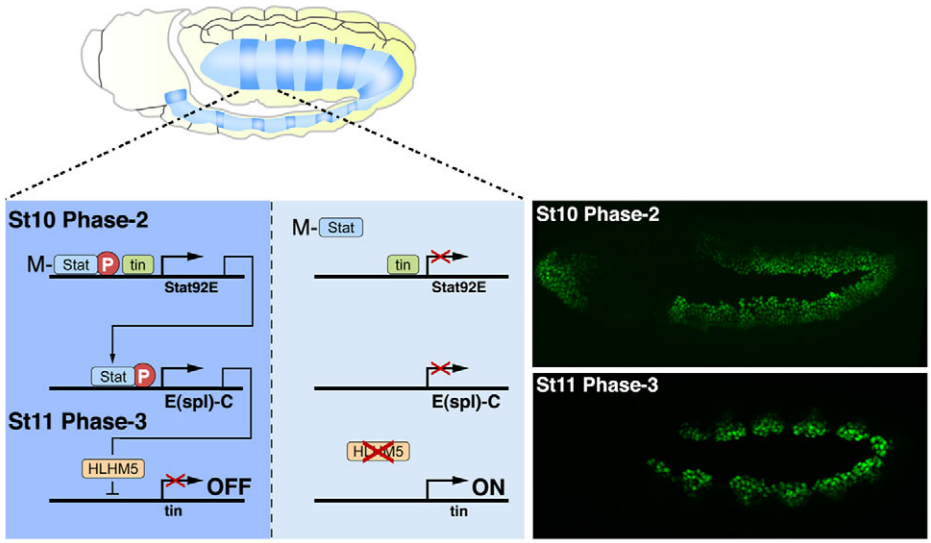

Fig. 7. JAK/Stat signaling regulates phase 3 *tin* expression. During St10, the JAK/Stat pathway is active in one region of each mesoderm segment (dark blue) and largely inactive in the opposing region (light blue). The Tin-responsive Stat92E mesoderm enhancer contains an SCBS (see Fig. S4 and Table S1 in the supplementary material) and directs segmental expression at St10 (Liu et al., 2009). Upd and Upd2 activate the JAK/Stat pathway and induce phosphorylation of maternally contributed Stat92E (M-Stat). Tin and M-Stat co-activate zygotic expression of *Stat92E*, which induces segmental expression of the E(spl)-C gene *HLHm5*. HLHm5 then represses *tin* to establish the phase 3 expression pattern in the dorsal mesoderm. *tin* expression is sustained in the region of the segment where JAK/Stat signaling is not active. Images on the right show Phase-2 and Phase-3 Tin expression. Embryos are oriented with anterior to the left.

Regulated *twi* expression directs cardiogenesis

Although the Twi target genes directing mesoderm development and subdivision have been studied in detail (Cripps et al., 1998; Sandmann et al., 2007; Yin et al., 1997), the molecular mechanism that restricts *twi* expression after gastrulation remains unclear. One regulator of *twi* is the Notch signaling pathway, which acts through E(spl)-C genes to restrict *twi* expression (Tapanes-Castillo and Baylies, 2004). However, Notch signaling appears to be active throughout the mesoderm after gastrulation. Our study suggests that segmented JAK/Stat signaling activity (Fig. 1H,I) differentially upregulates E(spl)-C gene expression in concert with Notch to produce periodic *twi* expression in the mesoderm (Fig. 5H,I). In addition, pan-mesodermal *twi* expression causes cardiac defects independently of cell fate specification (Fig. 6C,D), suggesting that the cardiac morphology defects in *Stat92E* embryos are due to dysregulated *twi* expression. These results highlight a previously unrecognized role for the JAK/Stat pathway and Twi in regulating cardiogenesis.

Sequential JAK/Stat-Dpp signals might regulate heart precursor diversification

Pericardial cell hyperplasia without a concomitant loss of cardioblasts has been reported for *dpp* hypomorphic embryos (Johnson et al., 2007) and *lame duck* (*lmd*) embryos (Sellin et al., 2009). A late Dpp signal, which occurs after the Dpp signal that regulates phase 2 *tin* expression, instructs the Gli-like transcription factor Lmd to repress Tin expression in fusion competent myoblasts (FCMs; Sellin et al., 2009). Tin expression appears to expand into the FCM domain in *Stat92E* embryos (see Fig. S2 in the supplementary material); however, the closest Stat92E chromatin binding domain is over 120 kb distal to the *lmd* transcriptional start site (see Table S1 in the supplementary material). Our study highlights the possibility that sequential JAK/Stat and then Dpp signals regulate Lmd function to direct heart precursor diversification.

E(spl) genes might be conserved Stat targets during mesoderm segmentation

In vertebrates, skeletal myogenesis initiates with the periodic specification of somites in the presomitic mesoderm (Gomez et al., 2008). Cyclical expression of *hairy1* in the chick, the hairy- and E(spl)-related family (Her) in zebrafish, and the orthologous Hes family in mice are under the control of Notch-Delta signaling (Giudicelli and Lewis, 2004). Loss of *her1* and *her7* alters the periodicity with which somite boundaries are specified in fish (Henry et al., 2002), and artificially stabilizing Hes7 causes somites to fuse in the mouse (Hirata et al., 2004). Thus, mesoderm segmentation is governed by Notch-Delta regulation of the E(spl)-C genes in both insects and vertebrates indicating that the two processes share molecular homology. A cell culture model of somitogenesis shows that oscillating *Hes1* expression is dependent on Stat activity (Hirata et al., 2002; Yoshiura et al., 2007). Our study supports the exciting possibility that JAK/Stat signaling and *E(spl)-C* form a conserved developmental cassette directing mesoderm segmentation throughout Metazoa.

Acknowledgements

We thank Erika Bach, Mary Baylies, Allison Bardin, Nobert Perrimon, Richard Cripps and the Bloomington Stock Center for fly stocks. We also thank Manfred Frasch, James Skeath and Bruce Paterson for antibodies.

Funding

This work was supported by the National Institutes of Health [2R01HL77439-05 to E.N.O.]; the Robert A. Welch Foundation; and a National Research Service Award fellowship [F32GM083530 to A.N.J.]. Deposited in PMC for release after 12 months.

Competing interests statement

The authors declare no competing financial interests.

Supplementary material

Supplementary material for this article is available at
http://dev.biologists.org/lookup/suppl/doi:10.1242/dev.071464/-/DC1

References

Bach, E. A., Vincent, S., Zeidler, M. P. and Perrimon, N. (2003). A sensitized genetic screen to identify novel regulators and components of the *Drosophila* janus kinase/signal transducer and activator of transcription pathway. *Genetics* **165**, 1149-1166.

Baeg, G. H., Zhou, R. and Perrimon, N. (2005). Genome-wide RNAi analysis of JAK/STAT signaling components in *Drosophila*. *Genes Dev.* **19**, 1861-1870.

Bardin, A. J., Perdigoto, C. N., Southall, T. D., Brand, A. H. and Schweisguth, F. (2010). Transcriptional control of stem cell maintenance in the *Drosophila* intestine. *Development* **137**, 705-714.

Bertet, C., Rauzi, M. and Lecuit, T. (2009). Repression of Wasp by JAK/STAT signalling inhibits medial actomyosin network assembly and apical cell constriction in intercalating epithelial cells. *Development* **136**, 4199-4212.

Callus, B. A. and Mathey-Prevot, B. (2002). SOCS36E, a novel *Drosophila* SOCS protein, suppresses JAK/STAT and EGF-R signalling in the imaginal wing disc. *Oncogene* **21**, 4812-4821.

Castanon, I., Von Stetina, S., Kass, J. and Baylies, M. K. (2001). Dimerization partners determine the activity of the Twist bHLH protein during *Drosophila* mesoderm development. *Development* **128**, 3145-3159.

Celniker, S. E., Dillon, L. A., Gerstein, M. B., Gunsalus, K. C., Henikoff, S., Karpen, G. H., Kellis, M., Lai, E. C., Lieb, J. D., MacAlpine, D. M. et al. (2009). Unlocking the secrets of the genome. *Nature* **459**, 927-930.

Cripps, R. M., Black, B. L., Zhao, B., Lien, C. L., Schulz, R. A. and Olson, E. N. (1998). The myogenic regulatory gene Mef2 is a direct target for transcriptional activation by Twist during *Drosophila* myogenesis. *Genes Dev.* **12**, 422-434.

Delidakis, C. and Artavanis-Tsakonas, S. (1992). The Enhancer of split [E(spl)] locus of *Drosophila* encodes seven independent helix-loop-helix proteins. *Proc. Natl. Acad. Sci. USA* **89**, 8731-8735.

Ekas, L. A., Baeg, G. H., Flaherty, M. S., Ayala-Camargo, A. and Bach, E. A. (2006). JAK/STAT signaling promotes regional specification by negatively regulating wingless expression in *Drosophila*. *Development* **133**, 4721-4729.

Giudicelli, F. and Lewis, J. (2004). The vertebrate segmentation clock. *Curr. Opin. Genet. Dev.* **14**, 407-414.

Gomez, C., Ozbudak, E. M., Wunderlich, J., Baumann, D., Lewis, J. and Pourquie, O. (2008). Control of segment number in vertebrate embryos. *Nature* **454**, 335-339.

Han, Z. and Olson, E. N. (2005). Hand is a direct target of Tinman and GATA factors during *Drosophila* cardiogenesis and hematopoiesis. *Development* **132**, 3525-3536.

Harrison, D. A., McCoon, P. E., Binari, R., Gilman, M. and Perrimon, N. (1998). *Drosophila* unpaired encodes a secreted protein that activates the JAK signaling pathway. *Genes Dev.* **12**, 3252-3263.

Henry, C. A., Urban, M. K., Dill, K. K., Merlie, J. P., Page, M. F., Kimmel, C. B. and Amacher, S. L. (2002). Two linked hairy/Enhancer of split-related zebrafish genes, her1 and her7, function together to refine alternating somite boundaries. *Development* **129**, 3693-3704.

Hirata, H., Yoshiura, S., Ohtsuka, T., Bessho, Y., Harada, T., Yoshikawa, K. and Kageyama, R. (2002). Oscillatory expression of the bHLH factor Hes1 regulated by a negative feedback loop. *Science* **298**, 840-843.

Hirata, H., Bessho, Y., Kokubu, H., Masamizu, Y., Yamada, S., Lewis, J. and Kageyama, R. (2004). Instability of Hes7 protein is crucial for the somite segmentation clock. *Nat. Genet.* **36**, 750-754.

Hombria, J. C., Brown, S., Hader, S. and Zeidler, M. P. (2005). Characterisation of Upd2, a *Drosophila* JAK/STAT pathway ligand. *Dev. Biol.* **288**, 420-433.

Hou, S. X., Zheng, Z., Chen, X. and Perrimon, N. (2002). The Jak/STAT pathway in model organisms: emerging roles in cell movement. *Dev. Cell* **3**, 765-778.

Jagla, K., Frasch, M., Jagla, T., Dretzen, G., Bellard, F. and Bellard, M. (1997). ladybird, a new component of the cardiogenic pathway in *Drosophila* required for diversification of heart precursors. *Development* **124**, 3471-3479.

Jiang, H., Patel, P. H., Kohlmaier, A., Grenley, M. O., McEwen, D. G. and Edgar, B. A. (2009). Cytokine/Jak/Stat signaling mediates regeneration and homeostasis in the *Drosophila* midgut. *Cell* **137**, 1343-1355.

Johnson, A. N., Burnett, L. A., Sellin, J., Paululat, A. and Newfeld, S. J. (2007). Defective decapentaplegic signaling results in heart overgrowth and reduced cardiac output in *Drosophila*. *Genetics* **176**, 1609-1624.

Karsten, P., Hader, S. and Zeidler, M. P. (2002). Cloning and expression of *Drosophila* SOCS36E and its potential regulation by the JAK/STAT pathway. *Mech. Dev.* **117**, 343-346.

Klinedinst, S. L. and Bodmer, R. (2003). Gata factor Pannier is required to establish competence for heart progenitor formation. *Development* **130**, 3027-3038.

Lai, E. C., Bodner, R. and Posakony, J. W. (2000). The enhancer of split complex of *Drosophila* includes four Notch-regulated members of the bearded gene family. *Development* **127**, 3441-3455.

Lilly, B., Zhao, B., Ranganayakulu, G., Paterson, B. M., Schulz, R. A. and Olson, E. N. (1995). Requirement of MADS domain transcription factor D-MEF2 for muscle formation in *Drosophila*. *Science* **267**, 688-693.

Liu, Y. H., Jakobsen, J. S., Valentin, G., Amarantos, I., Gilmour, D. T. and Furlong, E. E. (2009). A systematic analysis of Tinman function reveals Eya and JAK-STAT signaling as essential regulators of muscle development. *Dev. Cell* **16**, 280-291.

Novak, U., Ji, H., Kanagasundaram, V., Simpson, R. and Paradiso, L. (1998). STAT3 forms stable homodimers in the presence of divalent cations prior to activation. *Biochem. Biophys. Res. Commun.* **247**, 558-563.

Oellers, N., Dehio, M. and Knust, E. (1994). bHLH proteins encoded by the Enhancer of split complex of *Drosophila* negatively interfere with transcriptional activation mediated by proneural genes. *Mol. Gen. Genet.* **244**, 465-473.

Olson, E. N. (2006). Gene regulatory networks in the evolution and development of the heart. *Science* **313**, 1922-1927.

Qian, L., Liu, J. and Bodmer, R. (2005a). Neuromancer Tbx20-related genes (H15/midline) promote cell fate specification and morphogenesis of the *Drosophila* heart. *Dev. Biol.* **279**, 509-524.

Qian, L., Liu, J. and Bodmer, R. (2005b). Slit and Robo control cardiac cell polarity and morphogenesis. *Curr. Biol.* **15**, 2271-2278.

Reim, I. and Frasch, M. (2005). The Dorsocross T-box genes are key components of the regulatory network controlling early cardiogenesis in *Drosophila*. *Development* **132**, 4911-4925.

Reim, I., Mohler, J. P. and Frasch, M. (2005). Tbx20-related genes, mid and H15, are required for tinman expression, proper patterning, and normal differentiation of cardioblasts in *Drosophila*. *Mech. Dev.* **122**, 1056-1069.

Sandmann, T., Jakobsen, J. S. and Furlong, E. E. (2006). ChIP-on-chip protocol for genome-wide analysis of transcription factor binding in *Drosophila melanogaster* embryos. *Nat. Protoc.* **1**, 2839-2855.

Sandmann, T., Girardot, C., Brehme, M., Tongprasit, W., Stolc, V. and Furlong, E. E. (2007). A core transcriptional network for early mesoderm development in *Drosophila melanogaster*. *Genes Dev.* **21**, 436-449.

Sellin, J., Drechsler, M., Nguyen, H. T. and Paululat, A. (2009). Antagonistic function of Lmd and Zfh1 fine tunes cell fate decisions in the Twi and Tin positive mesoderm of *Drosophila melanogaster*. *Dev. Biol.* **326**, 444-455.

Silver, D. L. and Montell, D. J. (2001). Paracrine signaling through the JAK/STAT pathway activates invasive behavior of ovarian epithelial cells in *Drosophila*. *Cell* **107**, 831-841.

Sotillos, S., Espinosa-Vazquez, J. M., Foglia, F., Hu, N. and Hombria, J. C. (2010). An efficient approach to isolate STAT regulated enhancers uncovers STAT92E fundamental role in *Drosophila* tracheal development. *Dev. Biol.* **340**, 571-582.

Stancato, L. F., David, M., Carter-Su, C., Larner, A. C. and Pratt, W. B. (1996). Preassociation of STAT1 with STAT2 and STAT3 in separate signalling complexes prior to cytokine stimulation. *J. Biol. Chem.* **271**, 4134-4137.

Tapanes-Castillo, A. and Baylies, M. K. (2004). Notch signaling patterns *Drosophila* mesodermal segments by regulating the bHLH transcription factor twist. *Development* **131**, 2359-2372.

Venkatesh, T. V., Park, M., Ocorr, K., Nemaceck, J., Golden, K., Wemple, M. and Bodmer, R. (2000). Cardiac enhancer activity of the homeobox gene tinman depends on CREB consensus binding sites in *Drosophila*. *Genesis* **26**, 55-66.

Ward, E. J. and Skeath, J. B. (2000). Characterization of a novel subset of cardiac cells and their progenitors in the *Drosophila* embryo. *Development* **127**, 4959-4969.

Xu, X., Yin, Z., Hudson, J. B., Ferguson, E. L. and Frasch, M. (1998). Smad proteins act in combination with synergistic and antagonistic regulators to target Dpp responses to the *Drosophila* mesoderm. *Genes Dev.* **12**, 2354-2370.

Yi, P., Johnson, A. N., Han, Z., Wu, J. and Olson, E. N. (2008). Heterotrimeric G proteins regulate a noncanonical function of septate junction proteins to maintain cardiac integrity in *Drosophila*. *Dev. Cell* **15**, 704-713.

Yin, Z., Xu, X. L. and Frasch, M. (1997). Regulation of the twist target gene tinman by modular cis-regulatory elements during early mesoderm development. *Development* **124**, 4971-4982.

Yoshiura, S., Ohtsuka, T., Takenaka, Y., Nagahara, H., Yoshikawa, K. and Kageyama, R. (2007). Ultradian oscillations of Stat, Smad, and Hes1 expression in response to serum. *Proc. Natl. Acad. Sci. USA* **104**, 11292-11297.

Zaffran, S., Reim, I., Qian, L., Lo, P. C., Bodmer, R. and Frasch, M. (2006). Cardioblast-intrinsic Tinman activity controls proper diversification and differentiation of myocardial cells in *Drosophila*. *Development* **133**, 4073-4083.

Table S1. Analysis of Stat92E ChIP-chip hits

Chromosome arm	Minimum bp	Maximum bp	Score	*Associated gene(s)
chrX	2901424	2902236	73.14	*Kirre*
chrX	4305309	4306239	78.69	*bifid*
chrX	4510490	4511774	247.42	*peb*
chrX	5492329	5493147	57.14	*Vsx-1*
chrX	7187996	7188776	52.33	*unc-119*
chrX	7212926	7213667	57.44	*Atg-5*
chrX	7785401	7786530	117.32	*CG18624*, *Nek2*
chrX	8544368	8545492	72.83	*oc*
chrX	8574772	8575908	98.3	*CG12772*, *CG11284*
chrX	11912286	11913620	151.36	*CG15735*, *Tango4*, *Chrac-16*, *regucalcin*
chrX	13474786	13475449	54.66	*Tango13*
chrX	18681811	18682777	93.37	*Pk17E*, *CG6961*
chrX	19114551	19115369	68.04	*CG7884*, *Muc18B*
chrX	19576637	19578171	202.17	*dome*
chrX	21210090	21210714	50	*flil*, *tty*
chr2L	2972197	2973177	81.52	*Rrp1*, *gTub23C*
chr2L	5239115	5239985	61.34	*tkv*
chr2L	5460973	5461815	57.68	*mid*
chr2L	6684090	6685093	90.2	*Nhe3*, *CG11327*
chr2L	7056072	7056773	54.68	*Mnn1*, *milt*
chr2L	8300304	8301304	57.39	*Sarcoglycan a*, *CG7870*
chr2L	8302317	8303286	82.61	*Sarcoglycan a*, *CG7870*
chr2L	8841120	8842596	97.8	None predicted
chr2L	9448764	9449388	55.24	*numb*
chr2L	13165100	13165802	62.46	*Sir-2*, *DnaJ-H*
chr2L	18143948	18145177	86.76	*Socs36E*
chr2L	18149636	18150869	113.15	*Socs36E*
chr2L	18151113	18152319	96.76	*Socs36E*
chr2L	19571687	19572777	78.21	*spitz*
chr2L	19575764	19577326	143.96	*spitz*
chr2R	4801397	4802105	59.27	*lin*, *Pgi*
chr2R	7084164	7085223	81.8	*shn*
chr2R	7085496	7087345	197.62	*shn*
chr2R	7415422	7416161	54.38	*en*
chr2R	9389481	9390497	90.54	*drk*, *mars*
chr2R	9448745	9449489	52.86	CG13334, CG13335
chr2R	9454395	9455951	81.58	CG13335
chr2R	9455952	9456565	66.41	CG13335
chr2R	9456907	9458882	116.91	CG13335
chr2R	14689728	14690949	87.5	l(2)08717
chr2R	14737858	14738557	53.35	CG15100, CG15084
chr2R	15549267	15549972	57.74	mir-6 family, CG11018
chr2R	16470820	16471875	80.15	mir-310 to mir-313
chr2R	17137846	17138824	63.55	CG18375
chr2R	17532909	17534085	77.43	CG10082
chr2R	18576939	18578313	133.66	*ppa*, *robo*
chr2R	20898906	20899774	55.43	*zip*, *uzip*
chr3L	199589	200291	51.45	*mri*, *rno*
chr3L	377687	378630	70.67	*trachealess*
chr3L	612998	614603	106.06	*Reg-2*
chr3L	620809	621663	57.28	None predicted
chr3L	621935	623182	123.15	*Reg-2*
chr3L	732741	733716	66	CG13897
chr3L	1348356	1349718	108.69	*Ptp61F*
chr3L	2588365	2589085	52.5	*Ama*
chr3L	2590543	2591289	54.41	*dos*
chr3L	3319083	3320303	90.14	CG12077, CG12016
chr3L	4229611	4230633	58.93	*ImpL2*
chr3L	6757473	6758361	56.23	CG32392
chr3L	6759861	6760926	77.07	CG32392
chr3L	7428029	7429177	76.04	*Rac2*, CG14835
chr3L	9065751	9066414	56.8	CG4911, CG4942
chr3L	10068389	10069013	52.69	None predicted
chr3L	12607406	12608069	53.28	*caup*
chr3L	15705142	15705924	67.32	CG42571
chr3L	16036196	16037921	145.62	*th*
chr3L	16045410	16046109	54.64	*mbs*, *th*
chr3L	16205919	16206543	50.51	CG13073
chr3L	16483690	16484769	64.78	*argos*, CG33158
chr3L	19026485	19027109	50.07	*nkd*
chr3L	19995465	19996089	52.13	*Tom20*, CG7668
chr3R	851107	852115	68.09	None predicted
chr3R	2586670	2587879	147.41	*bcd*, *Ama*

chr3R	2826080	2826902	65.03	*Antp*
chr3R	5873670	5874811	127.75	CG12811, CG3925
chr3R	9724575	9725603	59.55	*ems*
chr3R	9735133	9736074	59.29	*ems*
chr3R	10818696	10819320	51.86	None predicted
chr3R	11847285	11848107	55.09	*GATAe*, CG17631
chr3R	13365487	13366458	69.38	*SF1*, *l(3)07882*
chr3R	14982574	14983546	59.78	*nos*, CG11779
chr3R	16375604	16376543	76.73	*Stat92E*
chr3R	16399505	16400659	126.86	CG5191, *TFAM*
chr3R	16460358	16461020	51.31	*Pi3K92E*, *Hairless*
chr3R	17466843	17468306	185.96	*E2F*
chr3R	18970976	18971681	53	*hh*, *unk*
chr3R	19947137	19947761	51.45	*Ac76E*, *CG42263*
chr3R	21853261	21854011	54.76	*m4*, *HLHm5*
chr3R	22692120	22693267	96.89	*ball*, *His2Av*
chr3R	26426808	26428152	161.49	CG2246, CG31019, CG31021

Data for this analysis was obtained from the modENCODE Stat92E chromatin immunopurification (ChIP)-chip study (Celniker et al., 2009).
*Includes all ESTs within 10 kb of the reported region